第 33 卷第 7 期 无 机 化 学 学 报 Vol.33 No.7
2017 年 7 月 CHINESE JOURNAL OF INORGANIC CHEMISTRY 1119-1131

含 C^N-螯合配体的环戊二烯基铱抗癌配合物

路小敏 田 梦 田珍珍 田来进 李梦琪 黄 静 刘 哲*
(曲阜师范大学化学与化工学院,抗癌药物开发与诊疗应用研究所,山东省生命有机分析重点实验室,
山东省绿色天然产物及医药中间体开发重点实验室,曲阜 273165)

摘要:合成、表征了 8 个半三明治结构环戊二烯基金属铱配合物[(η^5-Cp^x)Ir(C^N)Cl],其中 Cp^x 分别为四甲基环戊二烯基(C_5Me_4H),五甲基环戊二烯基(Cp*),四甲基(苯基)环戊二烯基(Cp^{xph}),四甲基(联苯)环戊二烯基(Cp^{xbiph}),C^N 为苯亚甲基甲胺(BIMA),*N*-(4-甲氧基苯亚甲基)苯胺(MBIA)。测定了其中 3 个配合物的单晶结构。所有配合物对 Hela 人宫颈癌细胞显示出很强的细胞毒性,IC_{50} 值为 1.7~32.9 μmol·L^{-1}。经检测 Cp^x 铱配合物的抗癌活性顺序为 Cp^{xbiph}>Cp^{xph}>C_5Me_4H>Cp*。配合物[(η^5-Cp^{xbiph})Ir(BIMA)Cl] (**A4**)和[(η^5-Cp^{xbiph})Ir(MBIA)Cl] (**B4**)表现出了最高的抗癌活性,比临床铂类药物顺铂活性高 4 倍以上。经检测,铱配合物 **A1**~**B4** 不与 9-甲基腺嘌呤和 9-乙基鸟嘌呤反应,与 pBR322 DNA 也没有作用,但这些配合物能够作为氢转移催化剂,将辅酶 NADH 转化为 NAD$^+$。机理研究表明配合物 **A4**、**B4** 处理 Hela 细胞时会引起明显的细胞凋亡和细胞周期的变化,并大幅增加细胞内活性氧(ROS)的水平。

关键词:半三明治配合物;环戊二烯基配体;铱;抗癌药物;ROS 水平;细胞凋亡;细胞周期;还原态烟酰胺腺嘌呤二核苷酸
中图分类号:O614.82$^+$5 **文献标识码**:A **文章编号**:1001-4861(2017)07-1119-13
DOI:10.11862/CJIC.2017.155

Potent Cyclopentadienyl Iridium Anticancer Complexes Containing C^N-chelating Ligands

LU Xiao-Min TIAN Meng TIAN Zhen-Zhen TIAN Lai-Jin LI Meng-Qi HUANG Jing LIU Zhe*
(*Institute of Anticancer Agents Development and Theranostic Application, Shandong Provincial Key Laboratory of Life-Organic Analysis, Shandong Provincial Key Laboratory of Pharmaceutical Intermediates and Analysis of Natural Medicine, Department of Chemistry and Chemical Engineering, Qufu Normal University, Qufu, Shandong* 273165, *China*)

Abstract: Half-sandwich cyclopentadienyl Ir(Ⅲ) complexes of the type [(η^5-Cp^x)Ir(C^N)Cl], (Cp^x=C_5Me_4H, Cp*, tetramethyl(phenyl)cyclopentadienyl (Cp^{xph}), tetramethyl(biphenyl)cyclopentadienyl (Cp^{xbiph}), C^N =*N*-benzylidenemethylamine (BIMA), *N*-(4-methoxybenzylidene)aniline (MBIA)), have been synthesized and characterized. X-ray crystal structures of three complexes have been determined. All complexes showed potent cytotoxicity, with IC_{50} values ranging from 32.9 to 1.7 μmol·L^{-1} toward Hela human cervical cancer cells. Their potency is in the trend: Cp^{xbiph}>Cp^{xph}>C_5Me_4H>Cp*. Complexes [(η^5-Cp^{xbiph})Ir(BIMA)Cl] (**A4**) and [(η^5-Cp^{xbiph})Ir(MBIA)Cl] (**B4**) displayed the highest potency, more than 4 times more active than the clinical platinum drug cisplatin. No binding to nucleobases 9-ethylguanine (9-EtG), 9-methyladenine (9-MeA) and pBR 322 DNA were detected. The ability of these iridium complexes to catalytic hydride transfer from the coenzyme NADH to NAD$^+$ is studied. Complexes **A4** and **B4** cause cell apoptosis and arrest cell cycles at G_1 phase when Hela cancer cells were treated with different IC_{50} concentrations of complexes, and increase the reactive oxygen species (ROS) dramatically, which appears to contribute to the anticancer activity. CCDC: 1528262, **A3**; 1528263, **B3**; 1538264, **dimer1**.

Keywords: half-sandwich complexes; cyclopentadienyl ligand; iridium; anticancer drug; ROS level; apoptosis; cell cycle arrest; NADH

收稿日期:2017-04-29。收修改稿日期:2017-05-19。
国家自然科学基金(No.21671118)和泰山学者工程资助项目。
*通信联系人。E-mail:liuzheqd@163.com

Chemotherapy with Pt complexes is one of the main pillars in the treatment of cancer today[1]. Despite their tremendous success, these platinum compounds suffer from two main disadvantages: they are inefficient against platinum-resistant tumors, and they have severe side effects such as nephron toxicity[2-3]. The clinical success and drawbacks of Pt anticancer drugs have stimulated the exploration of other metal-based anticancer compounds[4], in particular other platinum complexes[5] and some group 8 metal complexes containing iron[6-8], ruthenium[9-12], rhodium[13-14], osmium[15], which showed promising anticancer activity both *in vitro* and *in vivo*.

Half-sandwich cyclopentadienyl (Cp^x) Ir complexes have been successfully applied in traditional domains encompassing organic transformations[16-18], catalysis[19-23]. Very recently, potential biological applications of iridium compounds have attracted much attention[24-27]. A number of Cp* Ir(Ⅲ) complexes of the type [(η^5-Cp*)Ir(XY)Cl]$^{0/+}$, where XY=N^N-bound 2,2-bipyridine (bpy) or N^O-bound ligands[28], have been reported to be inactive toward A2780 human ovarian cancer cells. However, the electronic and steric properties of the ligands can have a major effect on the chemical and biological activities of transition metal complexes. We reported that the potency toward cancer cells increased with additional phenyl substitution on Cp*, and the anticancer activity can be improved significantly by replacement of one atom, changing neutral N^N-chelating ligand (bpy) with negatively charged C^N-chelating ligand 2-phenylpyridine (phpy), which leading to increased cellular uptake and nucleobase binding[29-30]. This finding has led us to make detailed investigations on Cp^x Ir(Ⅲ) complexes with C^N-bound ligands and to study the influence of phenyl- or biphenyl- substituted Cp* on their chemical and biological properties.

Oxidative stress caused by the generation of reactive oxygen species (ROS) is an effective method of killing cancer cells. ROS are produced in a wide range of physiological processes, in particular by mitochondria, and play valuable roles in cellular signaling. Such stress would have a smaller effect on redox control in normal cells. Organometallic iridium (Ⅲ) complexes and copper (Ⅱ) complexes have been reported to be effective ROS inducer[31-33].

In the work reported here, eight half-sandwich complexes of the type (η^5-Cp^x)Ir(C^N)Cl, where Cp^x is tetramethylcyclopentadienyl (C_5Me_4H), Cp*, tetramethyl (phenyl)cyclopentadienyl (Cp^{xph}) or tetramethyl (biphenyl)cyclopentadienyl (Cp^{xbiph}), and the C,N-chelating ligands are *N*-benzylidenemethylamine (BIMA) and *N*-(4-methoxybenzylidene)aniline (MBIA) (Chart 1), were designed, synthesized and characterized, and their antiproliferative activity against cancer cells and mechanism of action was investigated. To the best of our knowledge, this appears to be the first report of C_5Me_4H iridium anticancer agents. The results suggest that this new class of organometallic Ir(Ⅲ) complexes is well suited for development as anticancer agents.

1 Experimental

1.1 Materials

$IrCl_3 \cdot 3H_2O$, butyllithium solution (1.6 mol·L^{-1} in hexane), 1,2,3,4,5-pentamethylcyclopentadiene (95%), 2, 3, 4, 5-tetramethyl-2-cyclopentenone (95%), phenylmagnesium bromide, 4-bromobiphenyl, trimethyl(2, 3, 4, 5-tetramethyl-2,4-cyclopentadien-1-yl)silane (97%), *N*-benzylidenemethylamine (BIMA), *N*-(4-methoxybenzylidene)aniline (MBIA), 9-ethylguanine and 9-methyladenine were purchased from Sigma-Aldrich. $Cp^{xph}H$[34], $Cp^{xbiph}H$[28], **dimer2**[35], **A2**[36] and **B2**[37] were prepared according to literature methods. For the biological experiments, DMEM medium, fetal bovine serum, penicillin/streptomycin mixture, trypsin/EDTA, and phosphate-buffered saline (PBS) were purchased from Sangon Biotech. Testing compounds was dissolved in DMSO and diluted with the tissue culture medium before use.

1.2 Instruments and methods

1.2.1 X-ray crystallography

All diffraction data were obtained on a Bruker Smart Apex CCD diffractometer equipped with graphite-monochromated Mo $K\alpha$ radiation (λ=0.071 073 nm). Absorption corrections were applied using SADABS[38] program. The crystals were mounted in oil and held at

Chart 1　Iridium cyclopentadienyl complexes studied in this work

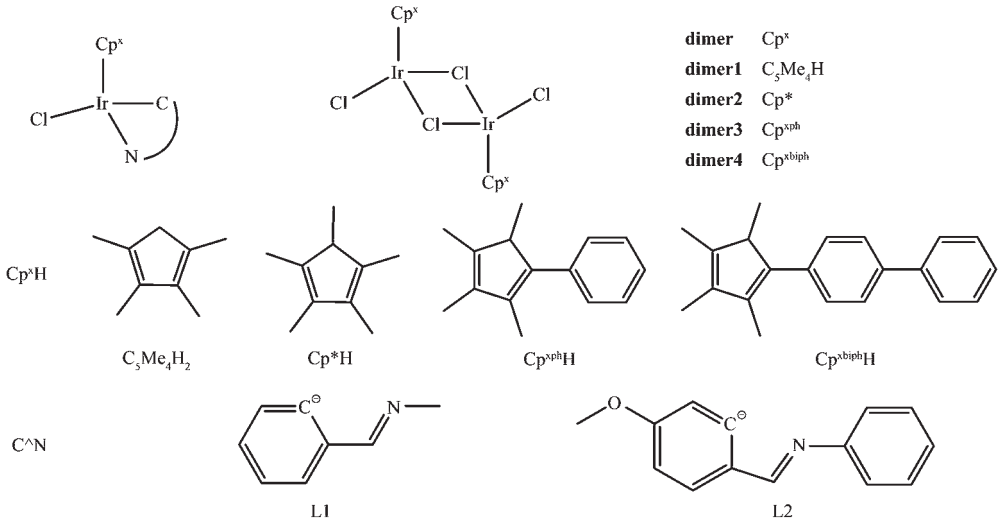

Complex	Cp^x	C^N
A1	C_5Me_4H	L1
A2	Cp*	L1
A3	Cp^{xph}	L1
A4	Cp^{xbiph}	L1
B1	C_5Me_4H	L2
B2	Cp*	L2
B3	Cp^{xph}	L2
B4	Cp^{xbiph}	L2

295 K with the Oxford Cryosystem Cobra. The structures were solved by direct methods using SHELXS (TREF)[39] with additional light atoms found by Fourier methods. Complexes **dimer1**, **A3** and **B3** were refined against F^2 using SHELXL, and hydrogen atoms were added at calculated positions and refined riding on their parent atoms. Crystallographic data are shown in Table S1, and selected bond lengths and angles are listed in Table S2.

CCDC: 1528262, **A3**; 1528263, **B3**; 1538264, **dimer1**.

1.2.2　Characterization

^{1}H NMR spectra were acquired at 298 K on Bruker -500 MHz spectrometers. ^{1}H NMR chemical shifts were internally referenced to $CDCl_3$ (δ 7.26) for chloroform-d_1, CHD_2OD (δ 3.33) for methanol-d_4. Electrospray ionization mass spectra (ESI-MS) were obtained on a Bruker Esquire 2000 ion trap spectrometer. For UV-Vis spectra, a TU-1901 UV-Vis recording spectrophotometer was used with 1 cm path-length quartz cuvettes (3 mL).

1.2.3　Reaction with NADH

The reaction of complexes **A1**~**B4** (*ca.* 0.8 μmol·L^{-1}) with NADH (87 μmol·L^{-1}, pH=6.7) in 5% (*V*/*V*) CH_3OH aqueous solution was monitored by UV-Vis at 298 K after 8 h. The reaction between complex **A2** (0.25 mmol·L^{-1}) and NADH (3.5 times the amount of complex) in CHD_2OD/D_2O (1∶1, *V*/*V*) at 298 K was detected by ^{1}H NMR. TON was calculated from the difference in NADH concentration after 8 h divided by the concentration of iridium catalyst. The concentration of NADH was obtained using the extinction coefficient ε_{339}=6 220 L·mol^{-1}·cm^{-1}.

1.2.4　Interactions with nucleobases

The reaction of complexes **A1**~**B4** (*ca.* 1 mmol·L^{-1}) with nucleobases typically involved addition of a solution containing 1 times the amount of nucleobase in D_2O to an equilibrium solution of complexes **A1**~**B4** in 40% (*V*/*V*) CHD_2OD/D_2O. ^{1}H NMR spectra of these solutions were recorded at 298 K after various

time intervals.

1.2.5 Cleavage plasmid DNA

Gel electrophoresis experiments were carried out with pBR 322 DNA, in 0.8% agarose solution, at 25 $V \cdot cm^{-1}$ for 1.5 h using TAE buffer (40 $mol \cdot L^{-1}$ Tris, 1 $mmol \cdot L^{-1}$ EDTA (disodium salt), pH 8.3). The pBR 322 DNA was stained with 0.5 $mg \cdot mL^{-1}$ GelRed. The cleavage reactions were quenched by the addition of bromophenol blue. The cleavage products were irradiated at room temperature with a UV lamp (590 nm).

1.2.6 Cell culture

Hela cervical carcinoma cells were obtained from Shanghai Institute of Biochemistry and Cell Biology (SIBCB) and were grown in Dubelco′s Modified Eagle Medium (DMEM). All media were supplemented with 10% fetal bovine serum, and 1% penicillin-streptomycin solution. All cells were grown at 310 K in a humidified incubator under a 5% (*V*/*V*) CO_2 atmosphere.

1.2.7 *In vitro* growth inhibition assay (MTT Assay)

After plating 5000 Hela cells per well in 96-well plates, the cells were preincubated in drug-free media at 310 K for 24 h before adding different concentrations of the compounds to be tested. In order to prepare the stock solution of the drug, the solid complex was dissolved in DMSO. This stock was further diluted using cell culture medium until working concentrations were achieved. The drug exposure period was 24 h. Subsequently, 15 μL of 5 $mg \cdot mL^{-1}$ MTT solution was added to form a purple formazan. Afterwards, 100 μL of dimethyl sulfoxide (DMSO) was transferred into each well to dissolve the purple formazan, and results were measured using a microplate reader (DNM-9606, Perlong Medical, Beijing, China) at an absorbance of 570 nm. Each well was triplicated and each experiment repeated at least three times. IC_{50} values are quoted as mean ±SEM.

1.2.8 Cell cycle analysis

Hela cells at 1.5×10^6 per well were seeded in a six-well plate. Cells were preincubated in drug-free media at 310 K for 24 h, after which drugs were added at concentrations of $0.25IC_{50}$, $0.5IC_{50}$, and IC_{50}. After 24 h of drug exposure, supernatants were removed by suction and cells were washed with PBS. Finally, cells were harvested using trypsin-EDTA and fixed for 24 h using cold 70% (*V*/*V*) ethanol. DNA staining was achieved by resuspending the cell pellets in PBS containing propidium iodide (PI) and RNAse. Cell pellets were washed and resuspended in PBS before being analyzed in a flow cytometer (ACEA NovoCyte, Hangzhou, China) using excitation of DNA-bound PI at 488 nm, with emission at 585 nm. The cell cycle distribution is shown as the percentage of cells containing G_0/G_1, S and G_2/M DNA as identified by propidium iodide staining.

1.2.9 Induction of apoptosis

Flow cytometry analysis of apoptotic populations of Hela cells caused by exposure to iridium complexes was carried out using the Annexin V-FITC Apoptosis Detection Kit (Beyotime Institute of Biotechnology, China) according to the supplier′s instructions. Briefly, Hela cells (7.5×10^5 per well) were seeded in a six-well plate. Cells were preincubated in drug-free media at 310 K for 24 h, after which drugs were added at concentrations of IC_{50} and $2IC_{50}$. After 24 h of drug exposure, cells were collected, washed once with PBS, and resuspended in 195 μL of Annexin V-FITC binding buffer which was then added to 5 μL of Annexin V-FITC and 10 μL of PI, and then incubated at room temperature in the dark for 15 min. Subsequently, the buffer placed in an ice bath in the dark. The samples were analyzed by a flow cytometer (ACEA NovoCyte, Hangzhou, China).

1.2.10 ROS determination

Flow cytometry analysis of ROS generation in Hela cells caused by exposure to iridium complexes was carried out using the Reactive Oxygen Species Assay Kit (Beyotime Institute of Biotechnology, Shanghai, China) according to the supplier′s instructions. Briefly, 1.5×10^6 Hela cells per well were seeded in a six-well plate. Cells were preincubated in drug-free media at 310 K for 24 h in a 5% (*V*/*V*) CO_2 humidified atmosphere, and then drugs were added at concentrations of $0.25IC_{50}$ and $0.5IC_{50}$. After 24 h of drug exposure, cells were washed twice with PBS and then incubated with the DCFH-DA probe (10 $\mu mol \cdot L^{-1}$) at 37 ℃ for 30 min, and then washed triple

immediately with PBS. The fluorescence intensity was analyzed by flow cytometry (ACEA NovoCyte, Hangzhou, China). At all times, samples were kept under dark conditions to avoid light-induced ROS production.

1.3 Synthesis

$[(\eta^5\text{-Cp}^{xph})IrCl_2]_2$ (**dimer3**). A solution of $Cp^{xph}H$ (1.0 g, 5.0 mmol) and $IrCl_3\cdot 3H_2O$ (0.5 g, 1.4 mmol) was pretreated with ultrasonic dissolving in an N_2 atmosphere and reacted with sonication in PTFE inner tank at 120 ℃ for 20 min and 150 ℃ for 20 min. The reaction mixture was allowed to cool to ambient temperature and pressure and the red-orange precipitate was filtered off. The volume of the dark red filtrate was reduced to *ca.* 15 mL on a rotary evaporator. Upon cooling to ambient temperature, an orange precipitate appeared which was collected by filtration. The product was washed with methanol and diethyl ether and dried in air. Yield: 0.45 g (58.5%). ^{1}H NMR (500 MHz, $CDCl_3$) δ 7.57 (dd, *J*=6.5, 3.0 Hz, 4H), 7.41~7.32 (m, 6H), 1.73 (s, 12H), 1.63 (s, 12H). Anal. Calcd. for $C_{30}H_{34}Ir_2Cl_4$ (%): C, 39.13; H, 3.72. Found(%): C, 39.14; H, 3.68.

$[(\eta^5\text{-Cp}^{xbiph})IrCl_2]_2$ (**dimer4**). The synthesis was performed as for **dimer3** using $Cp^{xbiph}H$ (0.5 g, 1.8 mmol) and $IrCl_3\cdot 3H_2O$ (0.2 g, 0.7 mmol). Yield: 0.13 g (35.8%). ^{1}H NMR (500 MHz, $CDCl_3$) δ 7.65 (d, *J*= 8.1 Hz, 4H), 7.62 ~7.48 (m, 8H), 7.45 (dd, *J*=15.1, 7.6 Hz, 4H), 7.36 (t, *J*=7.3 Hz, 2H), 1.75 (s, 12H), 1.70 (d, *J*=12.5 Hz, 12H). Anal. Calcd. for $C_{42}H_{42}Ir_2Cl_4$(%): C, 47.01; H, 3.95. Found(%): C, 46.87; H, 3.75.

$[(\eta^5\text{-}C_5Me_4H)IrCl_2]_2$ (**dimer1**). The synthesis was performed as for **dimer3** using trimethyl (2,3,4,5-tetramethyl-2,4-cyclopentadien-1-yl)silane (0.7 mL, 3 mmol) and $IrCl_3\cdot 3H_2O$ (0.33 g, 1.0 mmol). Yield: 0.17 g (18.4%). ^{1}H NMR (500 MHz, $CDCl_3$) δ 5.27 (s, 2H), 1.68 (s, 12H), 1.63 (s, 12H). Anal. Calcd. for $C_{18}H_{26}Ir_2Cl_4$ (%): C, 28.13; H, 3.41. Found: C, 28.25; H, 3.56.

$[(\eta^5\text{-}C_5Me_4H)Ir(BIMA)Cl]$ (**A1**). A solution of chloride complex **dimer1** (46.5 mg, 0.06 mmol), *N*-benzylidenemethylamine (14.3 mg, 0.12 mmol), and sodium acetate (49.2 mg, 0.6 mmol), and benzaldehyde (trace) in 20 mL of CH_2Cl_2 was stirred for 5 h at ambient temperature in N_2 atmosphere. The solution was filtered through celite. The filtrate was evaporated to dryness on a rotary evaporator and washed with diethyl ether and hexane. The product was recrystallized from CH_3OH. Yield: 19 mg (35.1%). ^{1}H NMR (500 MHz, $CDCl_3$) δ 8.25 (s, 1H), 7.84 (d, *J*=7.6 Hz, 1H), 7.52 (d, *J*=7.5 Hz, 1H), 7.13 (s, 1H), 6.98 (s, 1H), 4.78 (s, 1H), 4.01 (s, 3H), 1.78 (d, *J*=6.9 Hz, 9H), 1.72 (s, 3H). MS (MeOH): *m*/*z*=508.1 ($[(\eta^5\text{-}C_5Me_4H)Ir(BIMA)Cl]+K^+$). Anal. Calcd. for $C_{17}H_{21}IrNCl$(%): C, 43.72; H, 4.53; N, 3.00. Found(%): C, 43.78; H, 4.44; N, 2.88.

$[(\eta^5\text{-Cp}^{xph})Ir(BIMA)Cl]$ (**A3**). The synthesis was performed as for **A1** using complex **dimer3** (46 mg, 0.05 mmol), *N*-benzylidenemethylamine (12 mg, 0.1 mmol), and sodium acetate (41 mg, 0.5 mmol), and benzaldehyde (trace). Yield: 38 mg (70.0%). ^{1}H NMR (500 MHz, $CDCl_3$) δ 8.26 (d, *J*=1.3 Hz, 1H), 7.62 (d, *J*=7.5 Hz, 1H), 7.53 (dd, *J*=7.5, 1.2 Hz, 1H), 7.39~7.28 (m, 5H), 7.08 (tt, *J*=13.0, 6.5 Hz, 1H), 6.98 (td, *J*=7.4, 1.0 Hz, 1H), 3.73 (d, *J*=1.3 Hz, 3H), 1.87 (s, 3H), 1.80 (d, *J*=1.4 Hz, 6H), 1.67 (s, 3H). MS (MeOH): *m*/*z*=583.8 ($[(\eta^5\text{-Cp}^{xph})Ir(BIMA)Cl]+K^+$). Anal. Calcd. for $C_{23}H_{25}IrNCl$(%): C, 50.86; H, 4.64; N, 2.58. Found(%): C, 50.82; H, 4.69; N, 2.53.

$[(\eta^5\text{-Cp}^{xbiph})Ir(BIMA)Cl]$ (**A4**). The synthesis was performed as for **A1** using complex **dimer4** (53 mg, 0.05 mmol), *N*-benzylidenemethylamine (12 mg, 0.1 mmol), and sodium acetate (41 mg, 0.5 mmol), and benzaldehyde (trace). Yield: 24 mg (38.8%). ^{1}H NMR (500 MHz, $CDCl_3$) δ 8.28 (d, *J*=1.2 Hz, 1H), 7.64 (dd, *J*=9.1, 7.7 Hz, 3H), 7.58 (d, *J*=8.3 Hz, 2H), 7.54 (d, *J*=7.5 Hz, 1H), 7.51~7.40 (m, 4H), 7.36 (t, *J*=7.4 Hz, 1H), 7.10 (td, *J*=7.5, 1.3 Hz, 1H), 6.99 (dd, *J*=7.4, 6.5 Hz, 1H), 3.77 (t, *J*=7.8 Hz, 3H), 1.88 (s, *J*=10.2 Hz, 3H), 1.84 (s, 3H), 1.81 (s, 3H), 1.72 (s, 3H). MS (MeOH): *m*/*z*=583.8 ($[C_{23}H_{25}IrNCl]+K^+$). Anal. Calcd. for $C_{29}H_{29}IrNCl$(%): C, 56.25; H, 4.72; N, 2.26. Found(%): C, 56.29; H, 4.77; N, 2.20.

$[(\eta^5\text{-}C_5Me_4H)Ir(MBIA)Cl]$ (**B1**). The synthesis was performed as for **A1** using complex **dimer1** (46.5 mg, 0.06 mmol), *N*-(4-methoxybenzylidene)aniline (25.5 mg, 0.12 mmol), and sodium acetate (49.2 mg, 0.6 mmol), and benzaldehyde (trace). Yield: 27 mg (48.3%). ^{1}H

NMR (500 MHz, $CDCl_3$) δ 8.23 (s, 1H), 7.66~7.57 (m, 3H), 7.43 (d, J=2.4 Hz, 1H), 7.37 (t, J=7.8 Hz, 3H), 7.28 (d, J=7.4 Hz, 1H), 6.61 (dd, J=8.4, 2.4 Hz, 1H), 3.91 (s, 3H), 1.62 (s, 3H), 1.56 (s, 3H), 1.53 (s, 3H), 1.44 (s, 3H). MS (MeOH): m/z=598.8 ([(η^5-C_5Me_4H)Ir(MBIA)Cl]+K^+). Anal. Calcd. for $C_{23}H_{25}IrNClO$(%): C, 49.41; H, 4.51; N, 2.51. Found(%): C, 49.47; H, 4.46; N, 2.56.

[(η^5-Cp^{xph})Ir(MBIA)Cl] (**B3**). The synthesis was performed as for **A1** using complex **dimer3** (46 mg, 0.05 mmol), *N*-(4-methoxybenzylidene)aniline (22 mg, 0.1 mmol), and sodium acetate (41 mg, 0.5 mmol), and benzaldehyde (trace). Yield: 47 mg (74.0%). ^{1}H NMR (500 MHz, $CDCl_3$) δ 8.22 (s, 1H), 7.58 (d, J=8.3 Hz, 1H), 7.50 (d, J=7.3 Hz, 2H), 7.39~7.28 (m, 7H), 7.23 (d, J=7.4 Hz, 1H), 7.06~7.02 (m, 1H), 6.57 (dd, J=8.4, 2.4 Hz, 1H), 3.61 (s, 3H), 1.70 (s, 3H), 1.48 (s, 6H), 1.35 (s, 3H). MS (MeOH): m/z=675.7 ([(η^5-Cp^{xph})Ir(MBIA)Cl]+K^+). Anal. Calcd. for $C_{29}H_{29}IrNClO$(%): C, 54.83; H, 4.60; N, 2.21. Found(%): C, 54.75; H, 4.50; N, 2.26.

[(η^5-Cp^{xbiph})Ir(MBIA)Cl] (**B4**). The synthesis was performed as for **A1** using complex **dimer4** (53 mg, 0.05 mmol), *N*-(4-methoxybenzylidene)aniline (22 mg, 0.1 mmol), and sodium acetate (41 mg, 0.5 mmol), and benzaldehyde (trace). Yield: 23 mg (32.3%). ^{1}H NMR (500 MHz, $CDCl_3$) δ 8.22 (s, 1H), 7.64~7.54 (m, 5H), 7.52 (dd, J=8.3, 1.1 Hz, 2H), 7.49~7.39 (m, 4H), 7.39~7.31 (m, 3H), 7.26~7.20 (m, 1H), 7.05 (dd, J=11.3, 7.1 Hz, 1H), 6.57 (dd, J=8.4, 2.4 Hz, 1H), 3.61 (d, J=5.3 Hz, 3H), 1.76 (d, J=6.8 Hz, 3H), 1.49 (s, 6H), 1.41 (s, 3H). MS (MeOH): m/z=675.7 ([$C_{29}H_{29}IrNOCl$]+K^+). Anal. Calcd. for $C_{35}H_{33}IrNClO$ (%): C, 59.10; H, 4.68; N, 1.97. Found(%): C, 59.18; H, 4.64; N, 1.92.

2 Results and discussion

2.1 Synthesis

dimer1, **dimer2**, **dimer3** and **dimer4** were synthesized by using a Tank Eco Initiator microwave synthesizer. Compared to the heating reflux method, the yield was improved effectively[28]. Eight Ir(Ⅲ) half-sandwich complexes (Chart 1) of the type [(η^5-Cp^x)Ir(C^N)Cl], where Cp^x is C_5Me_4H, Cp* or its phenyl (Cp^{xph}) or biphenyl (Cp^{xbiph}) derivatives, and the C^N-chelating ligands are *N*-benzylidenemethylamine (BIMA) and *N*-(4-methoxybenzylidene)aniline (MBIA), were synthesized by reaction of the C^N-chelating ligands with the iridium precursors **dimer1**~**dimer4** in dichloromethane in the presence of sodium acetate as a base. All of the synthesized complexes were fully characterized by ^{1}H NMR spectroscopy, mass spectrometry and elemental analysis. Introduction of phenyl substituents on the Cp* ring decreased the reaction yields significantly. At the beginning, an iridium silane dimer [(η^5-$C_5Me_4SiMe_3$)$IrCl_2$]$_2$ was tried to synthesized by reaction of trimethyl(2,3,4,5-tetramethyl-2,4-cyclopentadien-1-yl)silane with $IrCl_3\cdot 3H_2O$ by microwave heating. Unfortunately, this method led to loss of silane with formation of **dimer1**.

2.2 X-ray crystal structures

The X-ray crystal structures of **dimer1**, **A3** and **B3** were determined. The structures and atom-numbering schemes are shown in Fig.1. Complexes **A3** and **B3** adopt the expected half-sandwich pseudo-octahedral "three-legged piano-stool" geometry with the iridium bound to a η^5-cyclopentadienyl ligand (Ir to ring centroid distances of 0.175 0, 0.182 2 and 0.183 1 nm, respectively). The Ir-Cl bond distances are 0.238 36(19), 0.239 21(10) and 0.240 30(9) nm for **dimer1**, **A3** and **B3**, respectively. The Ir-C (chelating ligand) bond lengths in **A3** and **B3** (0.203 7(4) and 0.203 3 (4) nm, respectively) are significantly shorter than the Ir-N bond lengths (0.208 4(3) and 0.209 5(3) nm, respectively).

The bond distances and angles in **dimer1** compare well to those found for the corresponding Cp* analogue **dimer2**[40]. The Ir-Cl(bridging)-Ir angle in **dimer1** is 1.11° more acute and the Cl(bridging)-Ir-Cl (bridging) angle in **dimer1** is 0.81° more obtuse, respectively, than those of the Cp* analogue. The Ir-Cl bound lengths in complex **A3** (0.239 21(10) nm) is slightly shorter than complex **B3** (0.240 30 (9) nm) (Table S2). The Ir-Cl bond length in **A3** (0.239 21(10) nm) is similar to that in **A2** (0.239 50(6) nm)[41]. The Ir-Cl bound length in complexes **B3** (0.240 30(9) nm) is similar to that in complex **B2** (0.240 38(5) nm)[37]. These results suggest that the introduction of phenyl

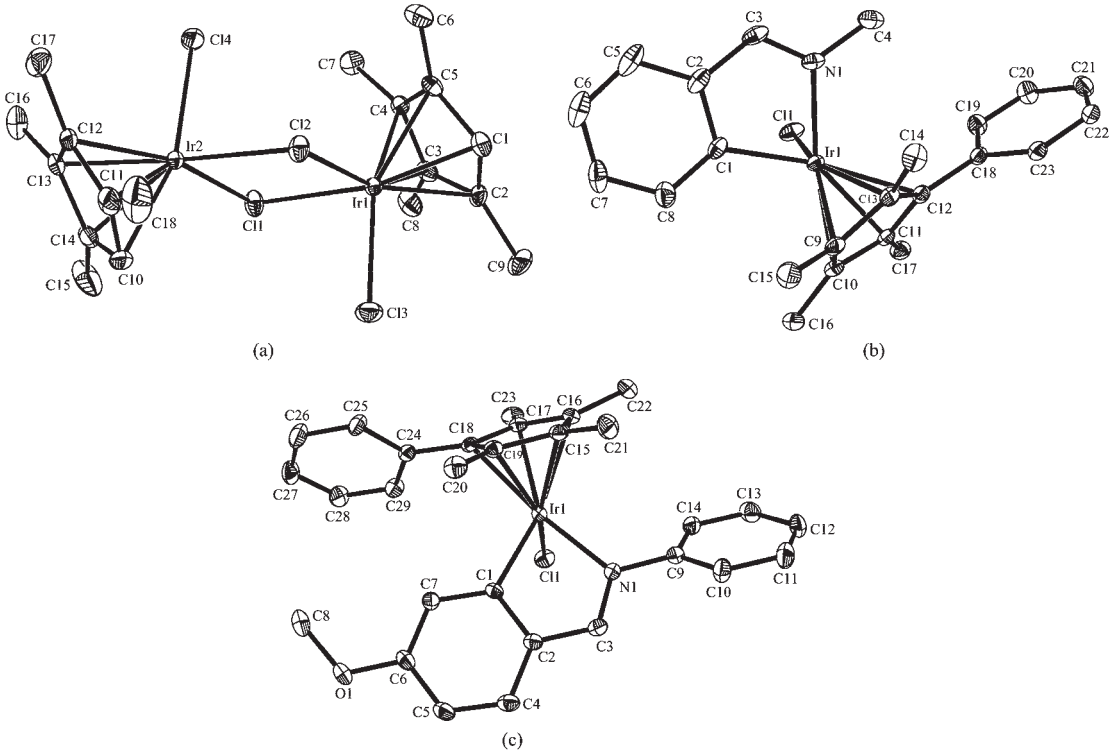

Hydrogen atoms have been omitted for clarity

Fig.1　X-ray crystal structures and atom-numbering schemes for complexes **dimer1**, **A3** and **B3** with thermal ellipsoids drawn at 50% probability

substituent on the Cp* ring does not give rise to significant change in structure.

2.3　Interaction with nucleobases

Because DNA is a potential target site for transition metal anticancer complexes, the binding of 9-ethylguanine (9-EtG) and 9-mehyladenine (9-MeA) to complexes **A1**~**B4** was studied. The addition of 1 times the amount of 9-MeA or 9-EtG to an equilibrium solution of **A1**~**B4** (1.0 mmol·L^{-1}) in 20% (*V*/*V*) MeOH-d_4 /D_2O at 298 K resulted in no additional ^{1}H NMR peaks over a period of 24 h (Fig.S1), indicating no reaction with 9-MeA or 9-EtG was observed for **A1**~**B4** (Table S3).

2.4　Cleavage plasmid DNA

The DNA binding ability of complexes **A1**~**B4** was studied through agarose gel electrophoresis[42] of supercoiled pBR 322 plasmid DNA[43] in Tris buffer. It is known that the binding of unwinding agents to the closed circular DNA can reduce its super helical density and hence decrease its rate of migration in agarose gel. However, for complexes **A1**~**B4**, no DNA cleavage was observed even at concentration of 100 μmol·L^{-1} (Fig.S2). Thus DNA is not likely to be a target for this type of complexes[31].

2.5　Antiproliferative activity

The activity of complexes **A1**~**B4** toward Hela human cervical cancer cells was investigated (Table 1). All of the eight complexes **A1**~**B4** were active, displaying IC_{50} values of 1.7~32.9 μmol·L^{-1}. C_5Me_4H

Table 1　Inhibition of growth of Hela human cervical cancer cells by complexes A1~B4 and cisplatin

Complex	IC_{50} / (μmol·L^{-1})
[(η^5-C_5Me_4H)Ir(BIMA)Cl] (**A1**)	13.0±0.5
[(η^5-Cp*)Ir(BIMA)Cl] (**A2**)	26.2±0.1
[(η^5-Cp^{xph})Ir(BIMA)Cl] (**A3**)	8.5±0.1
[(η^5-Cp^{xbiph})Ir(BIMA)Cl] (**A4**)	1.7±0.1
[(η^5-C_5Me_4H)Ir(MBIA)Cl] (**B1**)	17.2±1.2
[(η^5-Cp*)Ir(MBIA)Cl] (**B2**)	32.9±1.7
[(η^5-Cp^{xph})Ir(MBIA)Cl] (**B3**)	3.5±0.1
[(η^5-Cp^{xbiph})Ir(MBIA)Cl] (**B4**)	1.7±0.3
Cisplatin	7.5±0.2

complexes **A1**, **B1** and Cp* complexes **A2**, **B2** showed good activity, displaying IC_{50} values of 13.0~32.9 μmol·L^{-1}. Complex **A3** containing Cp^{xph} showed similar activity compare to cisplatin (IC_{50}=7.5 μmol·L^{-1}). Cp^{xbiph} complexes **A4**, **B4** and **B3** exhibited potent anticancer activity with IC_{50} values of 1.7~3.5 μmol·L^{-1}, respectively, *ca.* two to four times more active than cisplatin against the Hela cell line. For all complexes, the trend of increasing of activity with increasing phenyl substitution was the same: Cp^{xbiph} > Cp^{xph} > C_5Me_4H > Cp*. The introduction of phenyl or biphenyl substituents onto the tetramethylcyclopentadienyl ring results in a significant increase in cytotoxicity compared to the parent Cp* complex. This result is consistent with our previously report[28,44]. Interestingly, however, loss of one methyl group on the Cp* almost doubled the antiproliferative activity. To the best of our knowledge, this appears to be the first report of C_5Me_4H iridium anticancer agents.

2.6 Reaction with NADH

Coenzyme NADH and NAD^+ plays a key role in numerous biocatalyzed processes. Previously, we have shown that NADH can donate a hydride to aqua Ir(Ⅲ) cyclopentadienyl complexes and can produce ROS H_2O_2 thus provide a pathway to an oxidant mechanism of action[33]. We have investigated whether complexes **A1**~**B4** react with NADH and thus provide a redox pathway. When NADH (3.5 times the amount of complex) was added to a 0.25 mmol·L^{-1} solution of complex **A2**, a sharp singlet at δ −16.67 was observed in the ^{1}H NMR spectrum within ten minutes; this resonance corresponds to the Ir(Ⅲ) hydrido complex **A2** (Fig.2a). Simultaneously, NADH was converted into its oxidized form NAD^+. These data suggest that complex

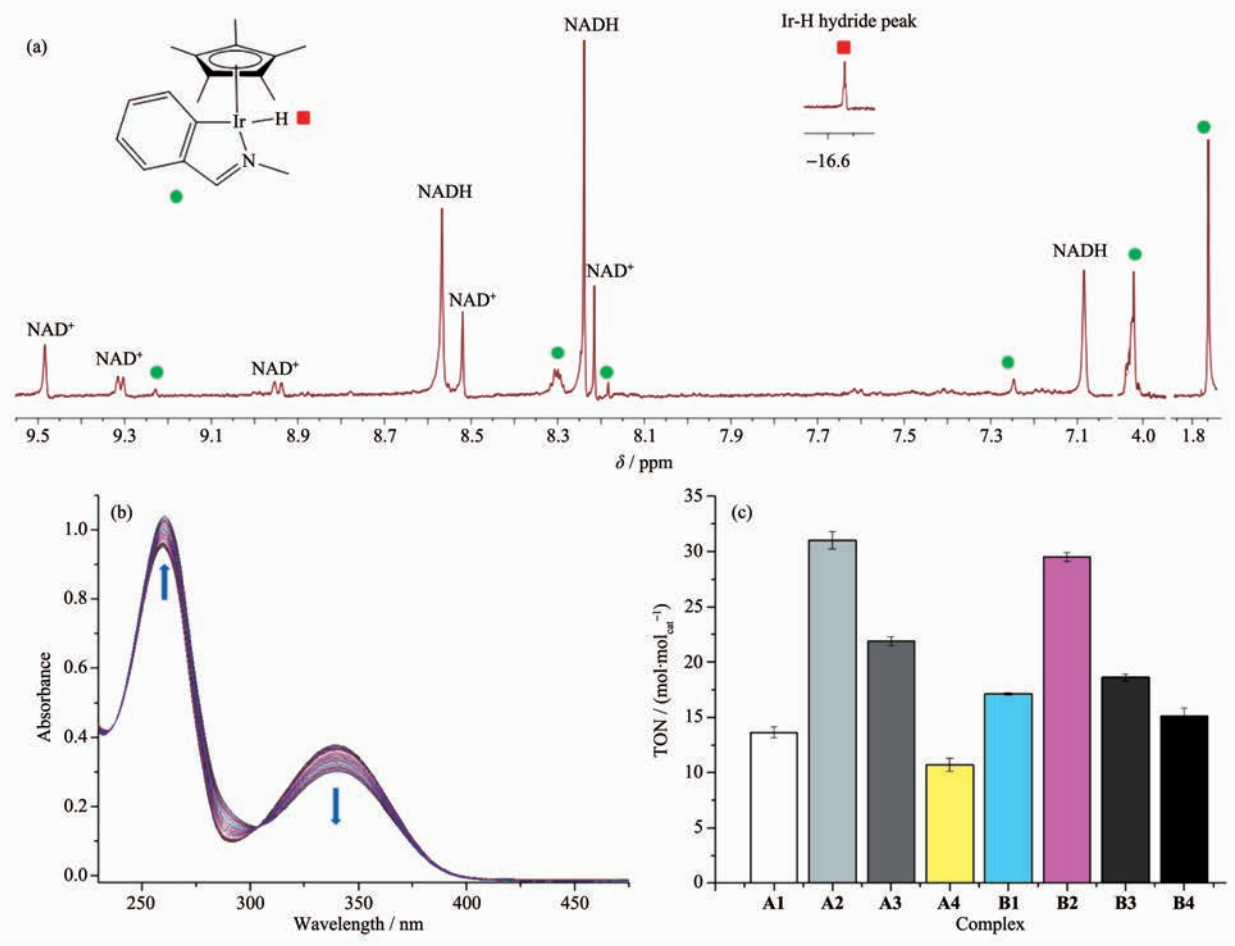

Fig.2 (a) ^{1}H NMR spectra for the reaction between complex **A2** (0.25 mm) and NADH (3.5 times the amount of complex) in CD_3OD/D_2O (1:1, *V*/*V*) at 298 K; (b) UV-Vis spectra for the reaction of NADH (87 μmol·L^{-1}) with complex **A2** (0.8 μmol·L^{-1}) in MeOH/H_2O (1.6:98.4, *V*/*V*) at 298 K for 8 h; (c) TONs of complexes **A1**~**B4**

A2 can accept a hydride from NADH. Similar results were obtained for the reaction of NADH with other complexes (Fig.S2). Strikingly, data from UV-Vis spectroscopy suggested that all the complexes can act as catalysts for hydride transfer from NADH (Fig.2b and Fig.S3). The turnover numbers (TON) in this work is defined as the amounts of NADH that a mole of catalyst can convert within 8 h. TONs of different complexes can be calculated by measuring the absorption difference at 339 nm (Fig.2c, Table S4). The maximum TON reached 31 $mol \cdot mol_{cat}^{-1}$ after 8 h for complex **A2**.

Previously, we have shown that organometallic iridium(Ⅲ) complexes are particularly effective oxidant catalysts which have anticancer activity, offering a new strategy for the design of metal-based anticancer drugs[33,45-46]. Other metal based compounds have also been reported to be effective biological catalysis [47]. For example, manganese macrocyclescan act as superoxide dismutase mimics and decompose superoxide into O_2 and H_2O_2 in cells[48]. Iron porphyrin complexes can catalyse the reduction of azides toimines[49], and copper peptide complexes can catalyse the degradation of RNA in hepatitis models[50]. Cobalt complexes, which cleave peptide bonds, can decompose amyloids present in diseases such as Alzheimer′s or Parkinson′s[51]. In particular, organometallic ruthenium compounds have shown success in the last few years. For example, Noyori-type catalytic transfer hydrogenation can be achieved in living cells, using Ru(Ⅱ) arene complexes with a chelated sulfonylethylamine ligand and formate as the hydride donor to convert coenzyme NAD^+ into NADH, and thereby modulate the NAD^+/NADH redox couple[52].

2.7 Cell cycle study

We performed cell cycle arrest analysis for complexes **A4** and **B4** toward Hela cells by flow cytometry to determine whether the induced cell growth inhibition was the result of cell cycle arrest. In comparison to the control population, the cell cycle progression was analyzed at concentrations of $0.25IC_{50}$, $0.5IC_{50}$ and IC_{50} of complexes **A4** and **B4** for 24 h. There was an increase in the G_1 proportion of Hela cell lines (from 55.0% to 68.0% and from 55.0% to 65.0%, respectively) (Fig.3, Table S5), indicating that the cells cycles were blocked in the G_1 phase.

2.8 Apoptosis assay

In order to investigate whether the reduction in cell viability observed by the MTT assay is based on apoptosis, Hela cells were treated with complexes **A4** and **B4** at equipotent concentrations of IC_{50} and $2IC_{50}$ for 24 h, then stained with Annexin V/propidium

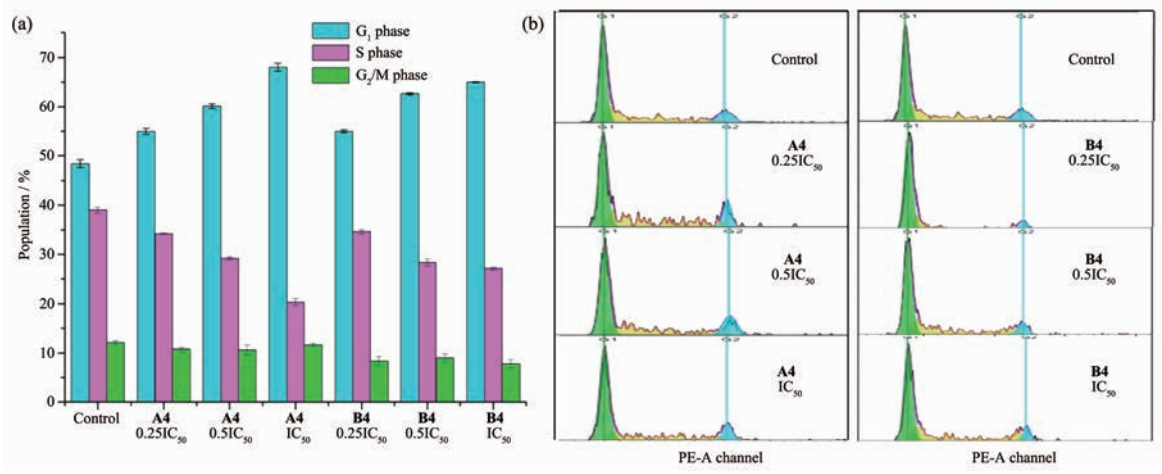

Concentrations used were equipotent at $0.25IC_{50}$, $0.5IC_{50}$ and IC_{50}; Cell staining for flow cytometry was carried out using PI/RNase; Data are quoted as mean ±SD of three replicates in (a)

Fig.3 Cell cycle analysis of Hela cells after 24 h of exposure to complexes **A4** and **B4** at 310 K; (a) Cell populations in each cell cycle phase for control (cells untreated) and complexes **A4** and **B4**; (b) FL2 histogram for control (cells untreated) and complexes **A4** and **B4**

iodide and analyzed by flow cytometry[53]. This allowed determination of cell populations as viable (unstained, only self-fluorescence), early apoptosis (stained by Annexin V only, green fluorescence), late apoptosis (stained by Annexin V and PI, green and red fluorescence), and nonviable (stained by PI only, red fluorescence). Upon exposure of the cells to complex **A4** at a concentration of IC_{50} after 24 h, only around 0.77% of Hela cells remained in early apoptotic phase and 4.95% of cells were in the late apoptotic phase (Fig.4 and Table S6). However, at $2IC_{50}$, a total of 26.16% (early apoptotic +late apoptotic) cells were undergoing apoptosis, whereas untreated cells remained 93.90% viable, indicating obvious induction

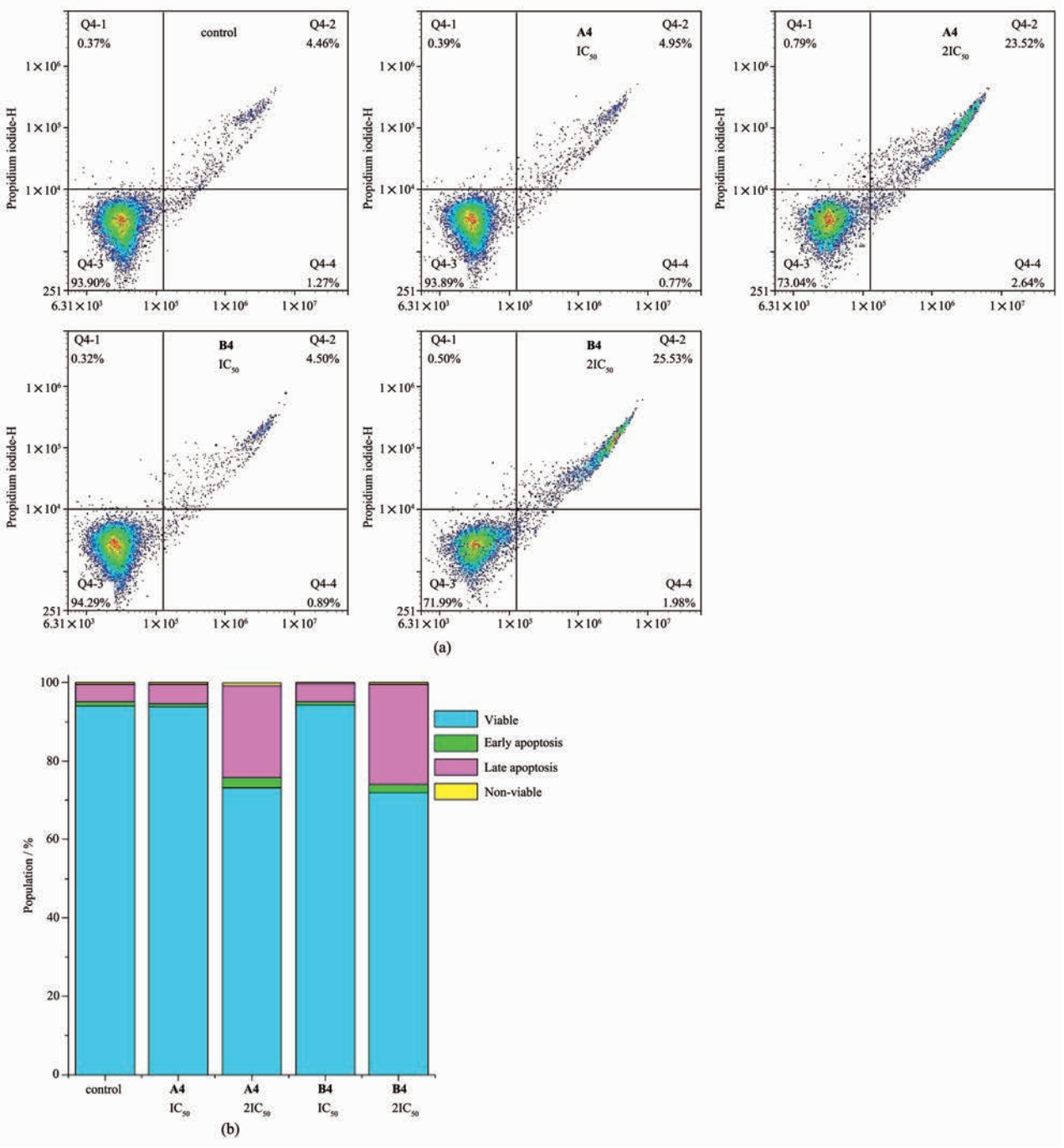

Fig.4 Apoptosis analysis of Hela cells after 24 h of exposure to complexes **A4** and **B4** at 310 K determined by flow cytometry using Annexin V-FITC vs PI staining at IC_{50} and $2IC_{50}$: (a) HeLa cells were control and treated with different concentrations of Ir(Ⅲ) complexes **A4** and **B4** for 24 h; (B) Populations for cells treated by **A4** and **B4**

of apoptosis at $2IC_{50}$. Similarly, apoptosis was observed when Hela cells were exposed to the complex **B4** at $2IC_{50}$ concentration, leading to a total of 27.51% (early apoptotic +late apoptotic) cells undergoing apoptosis. This suggested that cell death was induced by **A4** and **B4** mainly through apoptosis

2.9 Induction of ROS in Hela cancer cells

Oxidative stress caused by the generation of reactive oxygen species (ROS) is an effective method of killing cancer cells[33]. We suggested previously that the antiproliferative mechanism for the iridium pyridine complex is related to ROS generation. Here we determined the level of reactive oxygen species (ROS) in Hela cells induced by complexes **A4** and **B4** at concentrations of $0.25IC_{50}$ and $0.5IC_{50}$ by flow cytometry fluorescence analysis (Fig.5, Table S7).

After 24 h of drug exposure, dramatic increases in ROS levels in cells treated with complexes **A4** and **B4** was observed. The majority of Hela cancer cells, more than 94%, were in a high ROS levels after exposure to both Ir complexes **A4** and **B4** even at concentration of $0.25IC_{50}$. The concentration dependence of ROS induction was not obvious. These increases in ROS levels may provide a basis for killing cancer cells.

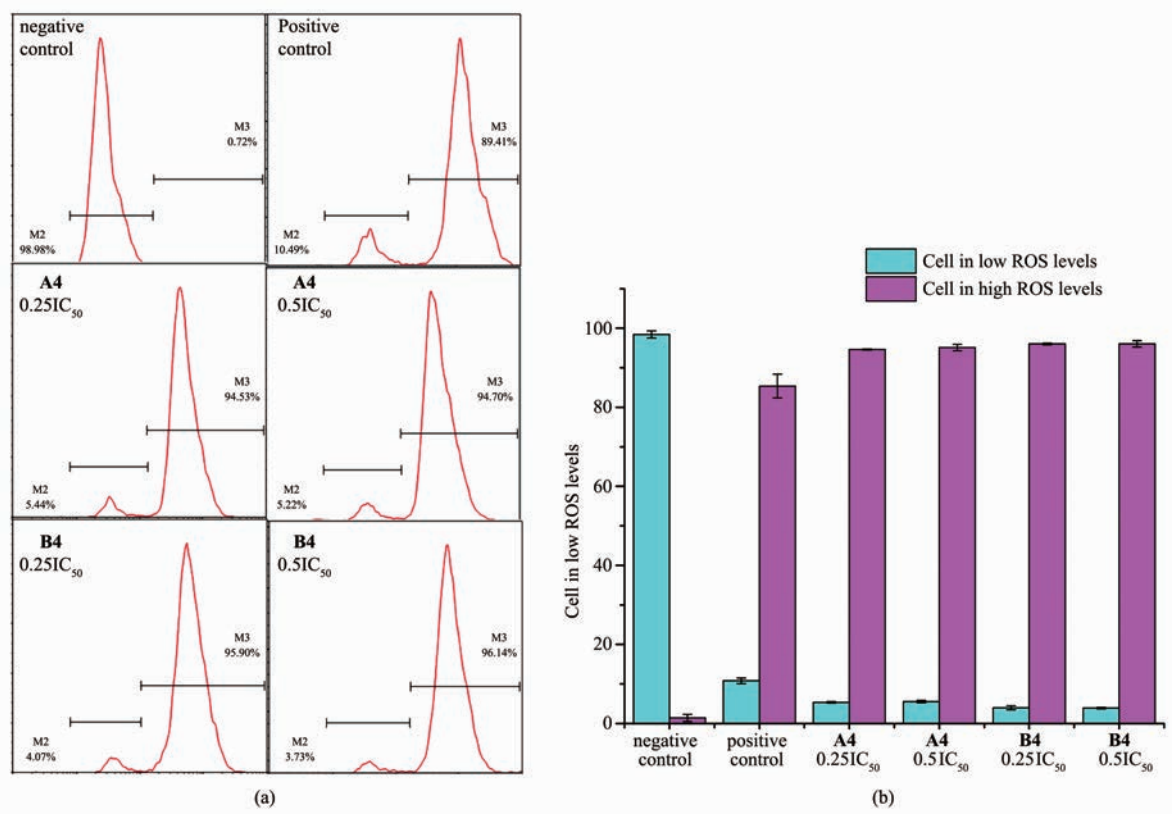

Data are quoted as mean±SD of three replicates in (b)

Fig.5 ROS induction in Hela cells treated with complexes **A4** and **B4** at equipotent concentrations of $0.25IC_{50}$ and $0.5IC_{50}$: (a) FL2 histogram for negative control (cells untreated), positive control and complexes **A4** and **B4**; (b) Populations for cells treated by **A4** and **B4**

3 Conclusions

In this work, we have prepared eight new organometallic Ir(Ⅲ) cyclopentadienyl complexes [(η^5-Cp^x)Ir(C^N)Cl] to explore the effect of cyclopentadienyl ligand and C^N-chelating ligand on their chemical and anticancer activity. The X-ray crystal structures of **dimer1**, **A3** and **B3** were determined. This appears to be the first report of C_5Me_4H iridium anticancer agents.

All complexes **A1**~**B4** studied here display high potency toward the human Hela cancer cell, comparable to, and for some complexes even higher

than the clinical anticancer drug cisplatin. The anticancer activity can be tuned by varying the cyclopentadienyl ligand, and increased in the order of Cp^{xbiph}> Cp^{xph}>C_5Me_4H >Cp*. The most active complexes **A4** and **B4** containing biphenyl substituent on cyclopentadienyl ring, is over 4 times more potent than cisplatin against Hela cells.

No distinct nucleobase binding for this type of complexes to 9-MeA and 9-EtG, and no unwinding to the pBR 322 DNA, suggesting that DNA could not be the main target for these complexes. However, all complexes are effective catalysis in transfer hydrogenation converting coenzyme NADH into NAD^+. Organometallic iridium complexes are unique in their ability to achieve such redox modulation in living cells[32]. In contrast to the DNA-targeting platinum drugs, these organometallic iridium complexes seem to offer the possibility of alternative redox mechanism of action. Complexes **A4** and **B4** induce a dramatic increase in the level of ROS in Hela cancer cells after 24 h. Additionally, cell cycle arrest at G_1 phase and distinct apoptosis were induced when Hela cancer cells were treated with different IC_{50} concentrations of complexes **A4** and **B4**. Our work suggests that this type of iridium complex could be a promising candidate for further evaluation as chemotherapeutic agents for human cancers.

Supporting information is available at http://www.wjhxxb.cn

References:

[1] Jakupec M A, Galanski M, Arion V B, et al. *Dalton Trans.*, **2008**:183-194

[2] Dyson P J and Sava G. *Dalton Trans.*, **2006**:1929-1933

[3] Wang X, Wang X, Guo Z. *Acc. Chem. Res.*, **2015**,**48**:2622-2631

[4] Gasser G, Ott I, Metzler-Nolte N. *J. Med. Chem.*, **2011**,**54**(1):3-25

[5] Wilbuer A, Vlecken D H, Schmitz D J, et al. *Angew. Chem. Int. Ed.*, **2010**,**49**(22):3839-3842

[6] Top S, Vessières A, Leclercq G, et al. *Chem. Eur. J.*, **2003**,**9**(21):5223-5236

[7] Hamels D, Dansette P M, Hillard E A, et al. *Angew. Chem. Int. Ed.*, **2009**,**121**(48):9124-9126

[8] Tan Y L K, Pigeon P, Hillard E A, et al. *Dalton Trans.*, **2009**:10871-10881

[9] Hartinger C G, Zorbas-Seifried S, Jakupec M A, et al. *J. Inorg. Biochem.*, **2006**,**100**(5/6):891-904

[10]Pierroz V, Joshi T, Leonidova A, et al. *J. Am. Chem. Soc.*, **2012**,**134**(50):20376-20387

[11]CHEN Xiang(陈相), CHAO Hui(巢晖), JI Ling-Nian(计亮年). *Chinese J. Inorg. Chem.*(无机化学学报), **2015**,**31**(9):1667-1677

[12]LI Hong(李红), CHAO Hui(巢晖), JING Xiong(蒋雄), et al. *Acta Phys.-Chim. Sin.*(物理化学学报), **2001**,**17**(8):728-732

[13]Dorcier A, Ang W H, Bolao S, et al. *Organometallics*, **2006**, **25**(17):4090-4096

[14]Markham J, Liang J, Levina A, et al. *Eur. J. Inorg. Chem.*, **2017**:1812-1823

[15]Zhou W, Wang X, Hu M, et al. *Chem. Sci.*, **2014**,**5**(7):2761-2770

[16]Davies D L, Al-Duaij O, Fawcett J, et al. *Organometallics*, **2010**,**29**(6):1413-1420

[17]Schwab P, Grubbs R H, Ziller J W. *J. Am. Chem. Soc.*, **1996**, **118**(1):100-110

[18]CHEN Yu(陈禹), DU Ke-Jie(杜可杰), CHAO Hui(巢晖), et al. *Prog. Chem.*(化学进展), **2009**,**21**(5):836-844

[19]GUO Li-Hua(郭丽华), CHEN Chang-Le(陈昶乐). *Sci. China*: *Chem.*(中国科学:化学), **2015**,**58**(11):1663-1673

[20]Guo L, Dai S, Chen C. *Polymers*, **2016**,**8**(2):37(10 pages)

[21]Xiong S Y, Guo L H, Zhang S M, et al. *Chin. J. Chem.*, **2017**,DOI:10.1002/cjoc.201600898

[22]Liu Z, Lebrun V, Kitanosono T, et al. *Angew. Chem. Int. Ed.*, **2016**:11587-11590

[23]Guo L, Jing X, Xiong S, et al. *Polymers*, **2016**,**8**(11):389(12 pages)

[24]Li S P-Y, Yip A M-H, Liu H-W, et al. *Biomaterials*, **2016**, **103**:305-313

[25]Lo K K-W. *Acc. Chem. Res.*, **2015**,**48**(12):2985-2995

[26]Zhao Q, Zhang C, Liu S, et al. *Sci. Rep.*, **2015**,**5**:16420(11 pages)

[27]Dörr M, Meggers E. *Curr. Opin. Chem. Biol.*, **2014**,**19**:76-81

[28]Liu Z, Habtemariam A, Pizarro A M, et al. *J. Med. Chem.*, **2011**,**54**(8):3011-3026

[29]Liu Z, Habtemariam A, Pizarro A M, et al. *Organometallics*, **2011**,**30**(17):4702-4710

[30]Liu Z, Romero-Canelón I, Habtemariam A, et al. *Organometallics*, **2014**,**33**(19):5324-5333

[31]Wang C, Liu J, Tian Z, et al. *Dalton Trans.*, **2017**,**46**:6870-6883

[32]Galluzzi L, Maiuri M C, Vitale I, et al. *Cell Death Differ.*,

2007,**14**(7):1237-1243

[33]Liu Z, Romero-Canelón I, Qamar B, et al. *Angew. Chem. Int. Ed.*, **2014**,**53**(15):3941-3946

[34]Bjrgvinsson M, Halldorsson S, Arnason I, et al. *J. Org. Chem.*, **1997**,**544**(2):207-215

[35]Tnnemann J, Risse J, Grote Z, et al. *Eur. J. Inorg. Chem.*, **2013**:4558-4562

[36]Davies D L, Al-Duaij O, Fawcett J, et al. *Dalton Trans.*, **2003**:4132-4138

[37]Li L, Brennessel W W, Jones W D. *Organometallics*, **2009**, **28**(12):3492-3500

[38]Sheldrick G M. *SADABS*, University of Göttingen, Germany, **1994**.

[39]Sheldrick G M. *Acta Crystallogr. Sect. A*, **1990**,**A46**:467-473

[40]Churchill M R, Julis S A. *Inorg. Chem.*, **1977**,**16**(6):1488-1494

[41]Li L, Brennessel W W, Jones W D. *J. Am. Chem. Soc.*, **2008**,**130**(37):12414-12419

[42]Wang J, Wang X, Song Y, et al. *Chem. Sci.*, **2013**,**4**(6):2605-2612

[43]Xi P X, Xu Z H, Chen F J, et al. *J. Inorg. Biochem.*, **2009**, **103**(2):210-218

[44]Liu Z, Sadler P J. *Acc. Chem. Res.*, **2014**,**47**:1174-1185

[45]Liu Z, Deeth R J, Butler J S, et al. *Angew. Chem. Int. Ed.*, **2013**,**52**:4194-4197

[46]Betanzos-Lara S, Liu Z, Habtemariam A, et al. *Angew. Chem. Int. Ed.*, **2012**,**51**:3897-3900

[47]Sasmal P K, Streu C N, Meggers E. *Chem. Commun.*, **2013**, **49**(16):1581-1587

[48]Filipovi M R, Koh A C W, Arbault S, et al. *Angew. Chem. Int. Ed.*, **2010**,**49**(25):4228-4232

[49]Sasmal P K, Carregal-Romero S, Han A A, et al. *ChemBioChem*, **2012**,**13**(8):1116-1120

[50]Bradford S, Cowan J A. *Chem. Commun.*, **2012**,**48**(25):3118-3120

[51]Lee T Y, Suh J. *Chem. Soc. Rev.*, **2009**,**38**(7):1949-1957

[52]Soldevila-Barreda J J, Romero-Canelón I, Habtemariam A, et al. *Nat. Commun.*, **2015**,**6**:6582

[53]WANG Jie(王洁), WANG Zeng-Li(王曾礼), ZHU Yuan-Jue(朱元珏), et al. *Chin. J. Intern. Med.*(中华内科杂志), **1998**(8):28-31